

## EPR study of electronic and magnetic properties of bis(*DL*- $\alpha$ -amino-*n*-butyrato) copper (II). A layered magnetic system

Rafael Calvo and Manuel A. Mesa

*Instituto Venezolano de Investigaciones Científicas, Centro de Física, Apartado 1827,  
Caracas 1010A, Venezuela*

(Received 24 January 1983)

Single crystals of the copper derivative of the amino acid *DL*- $\alpha$ -amino-*n*-butyric acid were studied by EPR at 300 K and 9.3 GHz. Only one exchange-narrowed line was observed for the two inequivalent copper ions in the lattice. The angular variation of its position and linewidth was measured in three perpendicular planes. The data on the position were used to obtain the molecular gyromagnetic factors and the orientation of the molecules within the unit cell. The angular variation of the linewidth shows an important contribution from spin diffusion, as is characteristic of two-dimensional magnetic systems. Anisotropic and antisymmetric exchange interactions contribute also to the linewidth. This two-dimensional behavior of bis(*DL*- $\alpha$ -amino-*n*-butyrato)Cu(II) is supported by existing data on the crystal structure of this salt. A lower limit for the exchange interaction between dissimilar copper ions in the lattice was obtained.

### I. INTRODUCTION

The study of transition-metal ions in biological systems is of interest for biologists as well as for physicists and chemists.<sup>1</sup> Electron paramagnetic resonance (EPR) spectroscopy has played an important role in these studies. In some cases, the information obtained is about the electronic structure of metal ions magnetically isolated within these structures. In other cases, the important goal is to learn about the magnetic interactions between metal ions. The role of the magnetic interactions in the biological properties is still unknown and it seems of great interest to search for their magnitudes and the possible paths which may transfer exchange interactions in a protein.

Metal derivatives of amino acids form crystalline structures which reproduce some of the characteristics of proteins and, at the same time, are simple enough to allow the use of the powerful techniques of solid-state physics in their study. Magnetic order has been observed below 0.117 K in the copper derivative of the amino acid *L*-isoleucine.<sup>2</sup> Also, the nickel derivative of glycine has easily detectable antiferromagnetic interactions between Ni atoms at a distance of 5.85 Å, and the exchange interaction between layers of Ni at a distance of about 10 Å is strong enough to produce three-dimensional order below 0.88 K.<sup>3,4</sup>

In this paper we report EPR measurements on single crystals of the copper derivative of the amino acid *DL*- $\alpha$ -amino-*n*-butyric acid. The position and the linewidth of the exchange-narrowed resonance was measured in three perpendicular planes, at 9.3 GHz, and room temperature. The information obtained allows us to learn about the electronic properties of the copper ions in the lattice and about the magnetic interactions between them.

The existing crystallographic data on the compound studied in this work are very incomplete, and are not sufficient to calculate the orientation of the molecules surrounding the two copper ions in the unit cell. However, we show here that our EPR study provides this information. Also, our data indicates a two-dimensional magnetic

behavior which is supported by the crystallographic data.

### II. EXPERIMENTAL PROCEDURES AND RESULTS

bis(*DL*- $\alpha$ -amino-*n*-butyrato) copper (II),



to be referred to as Cu(AAB)<sub>2</sub>, was obtained from the reaction of *DL*- $\alpha$ -amino-*n*-butyric acid with basic copper carbonate. Single crystals were obtained at room temperature by slow evaporation of a water solution. Chemical analysis by mass spectrometry, and x-ray diffraction measurements in powders, identified this compound with that reported by Stosick<sup>5</sup> in his early x-ray diffraction work.

The crystals grow in thin plates parallel to the *bc* plane with well-defined  $\hat{b}$  directions, simplifying the orientation of the sample. A Varian *E*-line EPR spectrometer working at 9.3 GHz with a previously described<sup>6</sup> microwave cavity was used. The sample was glued to an *L*-shaped sample holder with the  $\hat{a}'$  ( $=\hat{b}\times\hat{c}$ ),  $\hat{b}$ , and  $\hat{c}$  crystal directions along its  $\hat{x}$ ,  $\hat{y}$ , and  $\hat{z}$  orthogonal axes, respectively. The sample holder was then positioned in a pedestal inside the microwave cavity, so the magnetic field of a 12-in. Varian magnet could be rotated in the three planes of the sample. Any misorientation of the sample was then smaller than 1° for any orientation of the magnetic field.

The EPR spectrum consisted of only one line. Its position and linewidth were measured at 10° intervals along 180° in the three principal planes of the sample, at room temperature. The results are displayed in Figs. 1 and 2. The values obtained for the gyromagnetic factors are in good agreement with, but are more accurate than, those reported by Yokoi *et al.*<sup>7,8</sup> obtained for a powder of the same material. A line-shape analysis was performed with the magnetic field along the  $\hat{a}'$  and  $\hat{b}$  crystal directions. Figure 3 is a comparison of the line shape observed at room temperature with the field along the  $\hat{a}'$  axis with the Lorentzian and Gaussian curves giving the best fit to the

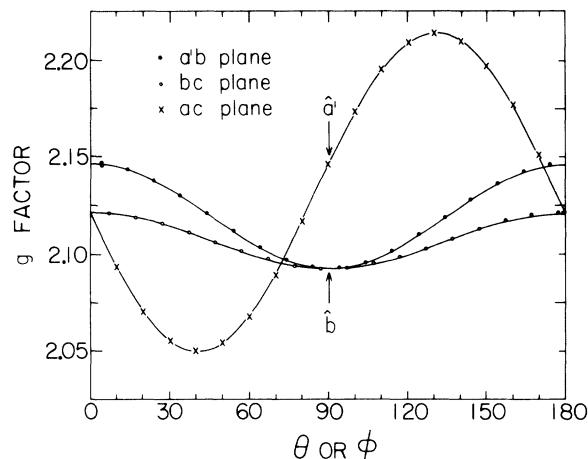


FIG. 1. Angular variation of the gyromagnetic factor measured at 300 K and 9.3 GHz in three orthogonal planes of a  $\text{Cu}(\text{AAB})_2$  single crystal. The solid lines are obtained with a least-squares fit of the data to a tensor  $\vec{g}^2$ , whose components are given in Table I.

data. It can be seen that the observed line shape is very close to a Lorentzian; a similar result is obtained for the field along the  $\hat{b}$  direction.

### III. DESCRIPTION OF THE CRYSTAL STRUCTURE

The crystal structure of  $\text{Cu}(\text{AAB})_2$  was reported by Stosick<sup>5</sup>; it forms monoclinic crystals belonging to the  $P2_1/c$  space group with  $a = 11.09 \text{ \AA}$ ,  $b = 5.06 \text{ \AA}$ ,  $c = 9.45 \text{ \AA}$ , and  $\beta = 87.85^\circ$ , and with two molecules  $\text{Cu}[\text{NH}_2\text{CH}(\text{CH}_2\text{CH}_3)\text{CO}_2]_2$  per unit cell. The available x-ray data is incomplete and gives only the  $x$  and  $z$  coordinates of all nonhydrogen atoms in the unit cell. The arrangement of the two amino-acid molecules around the copper ions is square planar and centrosymmetric with one amino nitrogen and one carboxyl oxygen of each amino-acid molecule bonded to the Cu atom. The distant

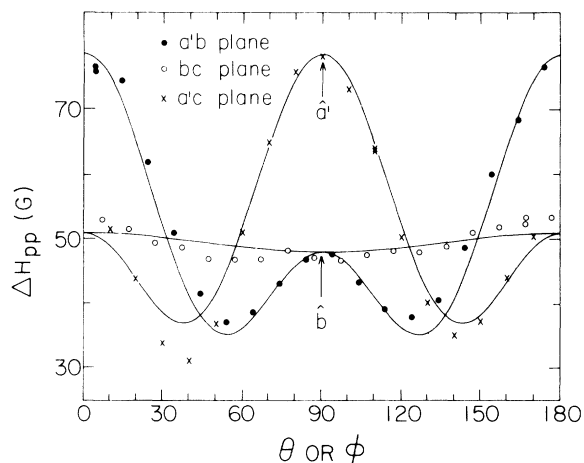


FIG. 2. Angular variation of the peak-to-peak linewidth measured at 300 K and 9.3 GHz in three orthogonal planes of a  $\text{Cu}(\text{AAB})_2$  single crystal. The solid lines are obtained from a least-squares fit of the data to Eq. 8.

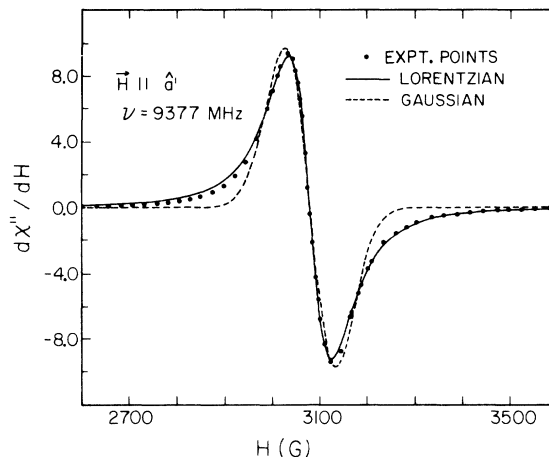


FIG. 3. Line-shape analysis for the magnetic field along the  $\hat{a}'$  direction. Experimental points for  $d\chi''/dH$  are compared with the field derivatives of Lorentzian and Gaussian curves giving the best fit to the data.

positions of the elongated octahedron are occupied by carboxyl oxygens of adjacent complexes. This copper complex is shown in Fig. 4. The two molecules in the unit cell of  $\text{Cu}(\text{AAB})_2$  are identical but rotated  $180^\circ$  around the  $\hat{b}$  axis. The copper atoms are in the centrosymmetric positions  $(0,0,0)$  and  $(0, \frac{1}{2}, \frac{1}{2})$ , in  $bc$  planes. The crystal can be visualized as layers of copper with nearest-neighbor distances of  $5.06 \text{ \AA}$  within layers and interlayer distances of  $11.09 \text{ \AA}$ , as shown in Fig. 5. It seems from our results that the closest electronic path between two nearest non-equivalent copper atoms is a hydrogen bond joining a carboxyl oxygen ligand of one copper with a nitrogen ligand of the other.

### IV. ANALYSIS OF THE EXPERIMENTAL DATA

#### A. The gyromagnetic factor

It is well known that when the exchange interaction between two dissimilar ions  $A$  and  $B$  in a crystal lattice is larger than the difference between their Zeeman energies, the EPR resonances of both types of ions collapse into a single resonance.<sup>9-13</sup> For each orientation  $\hat{h}$  of the magnetic field  $\vec{H}$ ,

$$\hat{h} = \vec{H} / |\vec{H}| = (\sin\theta \cos\phi, \sin\theta \sin\phi, \cos\theta),$$

the position of the single resonance is determined by a gyromagnetic factor  $g(\theta, \phi)$ , which is the arithmetical

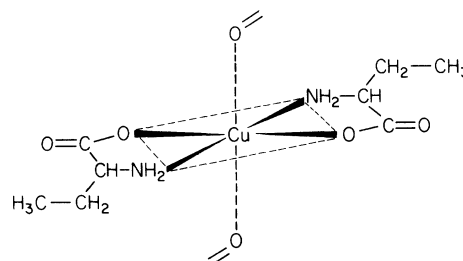


FIG. 4. View of a bis( $DL$ - $\alpha$ -amino- $n$ -butyrate) $\text{Cu}(\text{II})$  molecule. The two axial carboxyl oxygen ligands are also shown.

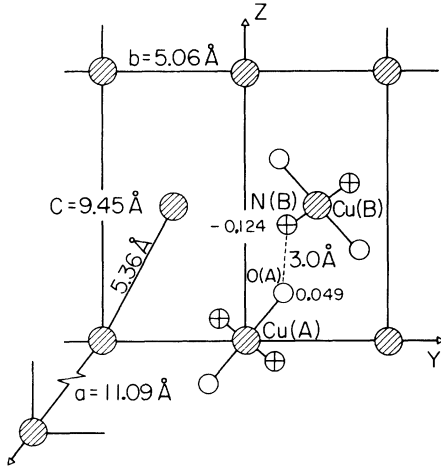


FIG. 5. View of the layered arrangement of Cu atoms in the  $\text{Cu}(\text{AAB})_2$  single crystals. Some of the oxygen and nitrogen nearest ligands of copper atoms at sites  $A$  and  $B$  are shown. There is a hydrogen bond joining a nitrogen ligand of one copper to the oxygen ligand of the other. This figure was drawn using the crystal data of Ref. 5 and our results for  $\theta_M$  and  $\phi_M$ .

mean of the gyromagnetic factors of ions in sites  $A$  and  $B$ :

$$g(\theta, \phi) = [g_A(\theta, \phi) + g_B(\theta, \phi)]/2. \quad (1)$$

$g_A(\theta, \phi) = (\hat{h} \cdot \vec{g}_A \cdot \vec{g}_A \cdot \hat{h})^{1/2}$  and  $g_B(\theta, \phi) = (\hat{h} \cdot \vec{g}_B \cdot \vec{g}_B \cdot \hat{h})^{1/2}$ , where  $\vec{g}_A$  and  $\vec{g}_B$  are the gyromagnetic tensors corresponding to the ions in sites  $A$  and  $B$ . It can be shown<sup>14</sup> that

$$g^2(\theta, \phi) = [g_A^2(\theta, \phi) + g_B^2(\theta, \phi)]/2 + [g_A^2(\theta, \phi) - g_B^2(\theta, \phi)]^2/16g^2(\theta, \phi), \quad (2)$$

where the first term on the right transforms like a second-order tensor, but the second term does not. When the second term in Eq. (2) is small, as happens in most cases,<sup>14</sup>  $g^2(\theta, \phi)$  transforms like the tensor

$$\vec{g}^2 = (\vec{g}_A^2 + \vec{g}_B^2)/2. \quad (3)$$

Since the sites  $A$  and  $B$  are related by a  $180^\circ$  rotation around the  $\hat{b}$  (or  $\hat{y}$ ) axis, the  $\vec{g}_A^2$  and  $\vec{g}_B^2$  tensors differ only in the sign of the  $xy$  and  $yz$  components when referred to the  $a', b, c$  ( $x, y, z$ ) system of axes, and the  $\vec{g}^2$  have zero  $xy$  and  $yz$  components, considering Eq. (3).

In order to learn about the electronic structure of  $\text{Cu}(\text{AAB})_2$ , we need to know the molecular  $\vec{g}_A^2$  and  $\vec{g}_B^2$  tensors instead of  $\vec{g}^2$  in Eq. (3). Two methods can be used to calculate the components of these molecular tensors from the experimental values of the components of  $\vec{g}^2$ .<sup>13,15</sup> In the first method, the principal molecular axis,

i.e., the orientation of the  $\text{Cu}(\text{AAB})_2$  molecules (shown in Fig. 4) within the unit cell, is used. Unfortunately, the existing crystallographic data do not allow us to calculate these orientations. In the second method, which we used to analyze our data, an assumption about the molecular tensors is made. For  $\text{Cu}(\text{II})$  in a square coordination of oxygens and nitrogens, it is very reasonable to assume axial symmetry for  $\vec{g}_A^2$  and  $\vec{g}_B^2$ , with  $g_\perp$  in the plane of the square of ligands and  $g_\parallel$  along its normal.<sup>16</sup>

Let us define  $(\theta_M, \phi_M)$  and  $(\pi - \theta_M, \pi - \phi_M)$  as the sets of polar and azimuthal angles corresponding to the normals  $\hat{n}_A$  and  $\hat{n}_B$  to the sites  $A$  and  $B$ , respectively. The molecular parallel directions with gyromagnetic factor  $g_\parallel$  are along these normals. The molecular gyromagnetic tensors  $\vec{g}_A^2$  and  $\vec{g}_B^2$  can be written in the  $xyz$  coordinate system in terms of  $g_\parallel$ ,  $g_\perp$ ,  $\theta_M$ , and  $\phi_M$ , and the tensor  $\vec{g}^2$  can be constructed, using Eq. (3), in terms of these parameters. The purpose is to calculate  $g_\parallel$ ,  $g_\perp$ ,  $\theta_M$ , and  $\phi_M$  from the experimental values of the four nonzero components of the symmetric tensor  $\vec{g}^2$  or its eigenvalues and eigenvectors. It is simple to show that

$$\begin{aligned} (g^2)_{xx} &= g_\perp^2 + (g_\parallel^2 - g_\perp^2) \cos^2 \epsilon_z \sin^2 \alpha, \\ (g^2)_{yy} &= g_\perp^2 \sin^2 \alpha + g_\parallel^2 \cos^2 \alpha, \\ (g^2)_{zz} &= g_\perp^2 + (g_\parallel^2 - g_\perp^2) \cos^2 \epsilon_x \sin^2 \alpha, \\ (g^2)_{xz} &= -(g_\parallel^2 - g_\perp^2) \cos \epsilon_x \cos \epsilon_z \sin^2 \alpha, \\ (g^2)_{xy} &= (g^2)_{yz} = 0. \end{aligned} \quad (4)$$

The eigenvalues with their corresponding eigenvectors are

$$\begin{aligned} (g^2)_1 &= g_\perp^2, \quad \hat{a}_1 = (\cos \epsilon_x, 0, \cos \epsilon_z), \\ (g^2)_2 &= g_\perp^2 \cos^2 \alpha + g_\parallel^2 \sin^2 \alpha, \quad \hat{a}_2 = (\cos \epsilon_z, 0, -\cos \epsilon_x), \\ (g^2)_3 &= g_\perp^2 \sin^2 \alpha + g_\parallel^2 \cos^2 \alpha, \quad \hat{a}_3 = (0, 1, 0), \end{aligned} \quad (5)$$

where  $\epsilon_x$  and  $\epsilon_z$  are the angles between  $\hat{n} = \hat{n}_A \times \hat{n}_B / |\hat{n}_A \times \hat{n}_B|$  and the  $\hat{x}$  and  $\hat{z}$  axes ( $\cos^2 \epsilon_z + \cos^2 \epsilon_x = 1$ ). By inspection of Eqs. (5) it can be seen that

$$g_\perp^2 = (g^2)_1, \quad g_\parallel^2 = (g^2)_2 + (g^2)_3 - (g^2)_1$$

and

$$\cos 2\alpha = [(g^2)_2 - (g^2)_3] / [(g^2)_2 + (g^2)_3 - 2(g^2)_1].$$

The angles  $\epsilon_x$  and  $\epsilon_z$  can be calculated from the eigenvectors of  $\vec{g}^2$  or by using Eqs. (4).

Our experimental data for  $g^2(\theta, \phi)$  shown in Fig. 1 was fitted to a  $\vec{g}^2$  tensor by a least-squares procedure and the agreement of the fit was excellent. No better agreement was obtained when a more general function was used, thus justifying Eq. (3). The values obtained for the com-

TABLE I. Values of the components of the  $\vec{g}^2$  tensor, obtained by a least-squares fit of the data in Fig. 1, and its eigenvalues and eigenvectors. The values are related to an orthogonal coordinate system where  $\hat{x} = \hat{a}'$ ,  $\hat{y} = \hat{b}$ , and  $\hat{z} = \hat{c}$ , and the data were taken at 300 K and 9.3 GHz.

$(g^2)_{xx} = 4.6063 \pm 0.0005$	$(g^2)_{yy} = 4.3805 \pm 0.0005$	$(g^2)_{zz} = 4.4997 \pm 0.0005$
$(g^2)_{xz} = -0.3475 \pm 0.0006$	$(g^2)_{xy} = (g^2)_{yz} = 0 \pm 0.0006$	
$(g^2)_1 = 4.2014 \pm 0.0007$	$\hat{a}_1 = (0.6513 \pm 0.0004, 0, 0.7588 \pm 0.0003)$	
$(g^2)_2 = 4.9046 \pm 0.0007$	$\hat{a}_2 = (0.7588 \pm 0.0003, 0, -0.6513 \pm 0.0004)$	
$(g^2)_3 = 4.3805 \pm 0.0005$	$\hat{a}_3 = (0, 1, 0)$	

ponents, the eigenvalues, and eigenvectors of  $\vec{g}^2$  are given in Table I. It can be observed in this table that the  $xy$  and  $yz$  components of the symmetric tensor  $\vec{g}^2$  are zero, as discussed before. The solid lines in Fig. 1 give the values calculated with the least-squares fit. Using the values of Table I together with Eqs. (4) and (5) we obtained

$$\begin{aligned} g_{||} &= 2.2547 \pm 0.0009, \quad g_{\perp} = 2.0497 \pm 0.0003, \\ 2\alpha &= 126.4^\circ \pm 0.1^\circ, \quad \epsilon_x = 49.4^\circ \pm 0.1^\circ, \\ \epsilon_z &= 40.6^\circ \pm 0.1^\circ. \end{aligned}$$

Also, a straightforward calculation allowed us to obtain the angles  $\theta_M$  and  $\phi_M$ , and the directions of the normals to the square of ligands of the copper atoms at the sites  $A$  and  $B$ . We found

$$\begin{aligned} \hat{n}_A &= (0.6774, 0.4507, -0.5814), \\ \hat{n}_B &= (-0.6774, 0.4507, 0.5814), \\ \theta_M &= 125.5^\circ \pm 0.5^\circ, \quad \phi_M = 33.6^\circ \pm 0.5^\circ. \end{aligned}$$

### B. The angular dependence of the linewidth

The magnetic dipolar interaction between magnetic ions broadens the EPR line and gives a contribution to the linewidth  $\Delta H$  which can be accurately calculated using Van Vleck's moment method<sup>17</sup> and the crystal data,

$$\Delta H = (M_{2d})^{1/2},$$

where  $M_{2d}$  is the dipolar contribution to the second moment of the resonance. When there is an isotropic exchange interaction between magnetic ions,

$$\mathcal{H}_{\text{ex}} = -J_0 \sum_{i,j} \vec{S}_i \cdot \vec{S}_j, \quad (6)$$

the line is narrowed by the exchange so that<sup>9-12</sup>

$$\Delta H = M_{2d}/J_0, \quad (7)$$

where appropriate units are used for  $M_{2d}$  and  $J_0$ .

It is known that the long-time behavior of the spin dynamic is governed by spin diffusion.<sup>18</sup> When this behavior is considered in the cases of one- and two-dimensional systems, it invalidates Eq. (7) and produces new contributions to the linewidth.<sup>19,20</sup> In particular, for layered two-dimensional systems it was proved<sup>20</sup> that this long-time spin-diffusive behavior gives a contribution proportional to  $(3 \cos^2 \theta_n - 1)^2$ , where  $\theta_n$  is the angle between the magnetic field and the normal to the layer. This contribution has been observed for  $\text{Mn}^{2+}$  in  $\text{K}_2\text{Mn}_4\text{F}_4$  (Ref. 20) and for  $\text{Cu}^{2+}$  in other lattices.<sup>21,22</sup> In the case of  $\text{Cu}^{2+}$  the spin-orbit interaction produces additional terms in the spin Hamiltonian. In particular, anisotropic and antisymmetric exchange interactions are important<sup>23</sup> and produce broadening of the EPR line.<sup>24</sup> In some two-dimensional systems these contributions compete with that produced by spin diffusion. They can be identified by their particular angular and temperature dependence.<sup>21,22,24</sup>

The analysis of Fig. 2 indicates that the main contribution to the observed angular variation of the peak-to-peak linewidth  $\Delta H$  is the isotropic one, and that expected from spin diffusion. The data was fitted to the function

$$\begin{aligned} \Delta H &= A + B(3 \cos^2 \theta_n - 1)^2 + C \sin^2 \theta_n \sin^2 \phi_n \\ &\quad + D \sin^2 \theta_n \cos^2 \phi_n, \end{aligned} \quad (8)$$

where  $\theta_n$  is the angle between the direction of the magnetic field and the  $\hat{a}'$  axis, the normal to the layers of Cu in  $\text{Cu}(\text{AAB})_2$ .  $\phi_n$  is measured in the  $bc$  plane, from the  $\hat{b}$  axis. The  $C$  and  $D$  terms were added to consider the small anisotropy of  $\Delta H$  in the  $yz$  plane, and it was proved that they improve the fit considerably. A least-squares calculation using Eq. (8) and the data in Fig. 2 gives the following values:  $A = 32.7 \pm 1.2$  G,  $B = 11.5 \pm 0.4$  G,  $C = 6.9 \pm 1.2$  G, and  $D = 4.0 \pm 1.2$  G. The contribution of the  $B$  term changes between 0 and 46 G with the angle, a contribution larger than the isotropic term ( $A$  term) for small  $\theta_n$ . The  $C$  and  $D$  terms give much smaller contributions, even when both terms are far from negligible.

## V. DISCUSSION AND CONCLUSIONS

It is interesting to analyze some general findings in Figs. 1 and 2. When the magnetic field moves in the  $a'b$  and  $bc$  planes, both the gyromagnetic factor and the linewidth have extrema for the magnetic field along the crystal axes, as required by the symmetry of the crystal. However, in the  $a'c$  plane, where there are no symmetry requirements, the angular dependence of the linewidth has clearly defined extrema along the axes  $\hat{a}'$  and  $\hat{c}$ , while the gyromagnetic factor does not. The positions of the extrema for  $g(\theta, \phi)$  in this plane are defined by  $\epsilon_x$  and  $\epsilon_z$  and depend on  $\theta_M$  and  $\phi_M$ , i.e., they reflect a structural property of  $\text{Cu}(\text{AAB})_2$ . The linewidth, however, reflects the magnetic properties of the compound. The maximum observed for  $\vec{H} \parallel \hat{a}'$  is telling us that the direction  $\hat{a}' = \hat{b} \times \hat{c}$  has some particular meaning for the magnetic properties. We have interpreted this result as a consequence of quasi-two-dimensional behavior of a layered compound, where  $\hat{a}'$  is the normal to the copper layers.

Unfortunately, there are no magnetic susceptibility measurements for  $\text{Cu}(\text{AAB})_2$  which can be used to evaluate  $J_0$  in Eq. (6). Since the magnetic resonance lines of copper ions at sites  $A$  and  $B$  collapse to a single resonance, Eq. (1) allows us to put a lower limit  $|J_0| \geq 0.03 \text{ cm}^{-1}$  on the exchange interaction between nearest copper ions at sites  $A$  and  $B$ . This conclusion is supported by our linewidth measurements: If the source of broadening is the magnetic dipolar interaction between Cu ions, it is simple to calculate the linewidths using the Van Vleck's moment method.<sup>17</sup> We obtained linewidths ranging between 154 and 340 G, with an angular behavior different from that observed. These values are at least a factor of 4 larger than those measured. Using Eq. (7) we conclude that a more reasonable lower limit for the exchange interaction between nearest dissimilar Cu ions at a distance of 5.36 Å is  $|J_0| \geq 0.12 \text{ cm}^{-1}$ . Since spin diffusion is the most important contribution to  $\Delta H$  we conclude that interlayer exchange interactions (between Cu ions at distances larger than 11 Å) are much smaller than this value. However, the fact that the observed line shape is very close to a Lorentzian curve tells us that these interlayer interactions are not negligible.<sup>21,24</sup> In the case of the  $\text{Cu}(\text{II})$  complex of  $L$ -isoleucine, Newman *et al.*,<sup>2</sup> using their magnetic susceptibility data, calculated a ferromagnetic exchange coupling constant  $J_0 = 0.084 \text{ cm}^{-1}$  between nearest Cu ions at

a distance of 6.1 Å. Also, they obtained an antiferromagnetic coupling constant  $J = -0.014 \text{ cm}^{-1}$  for the interlayer coupling constant. In  $\text{Cu}(\text{AAB})_2$  the distance is smaller,  $d_{A-B} = 5.36 \text{ Å}$ , and then our result for  $|J_0|$  seems to be very reasonable.

The relative importance of the  $C$  and  $D$  terms in Eq. (8) tells us that anisotropic and antisymmetric exchange interactions cannot be neglected in  $\text{Cu}(\text{AAB})_2$  and, as has been observed for other systems,<sup>21</sup> they give contributions to the linewidths which compete with those originated by spin diffusion. It is impossible, however, to evaluate these contributions from the existing data.

Our measurements of the gyromagnetic factor analyzed before give information about the electronic and structural properties of the compound.<sup>16</sup> The values obtained for  $g_{\parallel}$  and  $g_{\perp}$  are typical for cupric ions in a square coordination of oxygens and nitrogens as that shown in Fig. 4, and indicate a  $d_{x^2-y^2}$  orbital ground state for the  $\text{Cu}(\text{II})$  ions in  $\text{Cu}(\text{AAB})_2$ . The values of  $\theta_M$  and  $\phi_M$  give, probably within 1°, the orientation of the  $\text{Cu}(\text{AAB})_2$  molecules within the unit cell. The existing structural data<sup>5</sup> do not allow us to prove this result, but  $\theta_M$  and  $\phi_M$  can be used together with the crystal data in order to learn about the chemical connection between Cu ions at sites  $A$  and  $B$ . Figure 5 is a projection of the crystal on the  $bc$  plane, the plane of the copper layers. It was constructed using the values for the  $x$  and  $z$  coordinates given by Stosick<sup>5</sup> for the oxygen and nitrogen atoms, together with our values of  $\theta_M$  and  $\phi_M$ . Approximate values for the  $y$  coordinates of the oxygen and nitrogen atoms bonded to the copper were

obtained and used to construct Fig. 5. This figure suggests that the closest path between Cu atoms at  $A$  and  $B$  is a hydrogen bond joining a nitrogen ligand of one copper to the oxygen ligand of the other. The nitrogen-to-oxygen distance of this hydrogen bond is about 3 Å. This path of three atoms could be the electronic path where the superexchange interaction between copper ions is transferred. A similar behavior was observed for the interaction between nearest Ni ions in nickel diglycine dihydrate.<sup>4</sup>

This investigation provides the first study of the magnetic properties of  $\text{Cu}(\text{AAB})_2$ , a layered compound for which spin diffusion is the main source of line broadening. It is evident that more experimental data, particularly magnetic susceptibility measurements at low temperatures, are needed to characterize the magnetic properties of this compound. We have shown that EPR measurements are useful to obtain information about the magnetic interactions and also about the chemical structure, even when magnetically undiluted samples are used. A careful theoretical analysis of the superexchange interactions in this and similar structures would be very helpful to learn about the magnetic interactions in complex macromolecules.

#### ACKNOWLEDGMENTS

The authors are grateful to Dr. Raul Abreu for a critical reading of the manuscript. This work was partially supported by el Consejo Nacional de Investigaciones Científicas y Tecnológicas (CONICIT), Venezuela.

- <sup>1</sup>A. S. Brill, *Transition Metal Ions in Biochemistry* (Springer, Berlin, 1977).
- <sup>2</sup>P. R. Newman, J. L. Imes, and J. A. Cowen, *Phys. Rev. B* **13**, 4093 (1976).
- <sup>3</sup>R. Calvo, O. R. Nascimento, M. Torikachvili, and M. B. Maple, *J. Appl. Phys.* **53**, 2671 (1982).
- <sup>4</sup>R. Calvo, O. R. Nascimento, Z. Fisk, J. Suassuna, S. B. Oseroff, and I. Machin, *J. Appl. Phys.* **53**, 2674 (1982).
- <sup>5</sup>A. J. Stosick, *J. Am. Chem. Soc.* **67**, 362 (1945).
- <sup>6</sup>R. A. Isaacson, C. Lulich, S. B. Oseroff, and R. Calvo, *Rev. Sci. Instrum.* **51**, 1409 (1980).
- <sup>7</sup>H. Yokoi, M. Sai, T. Isobe, and S. Oshawa, *Bull. Chem. Soc. Jpn.* **45**, 2189 (1972).
- <sup>8</sup>H. Yokoi, *Bull. Chem. Soc. Jpn.* **47**, 639 (1974).
- <sup>9</sup>P. W. Anderson and P. R. Weiss, *Rev. Mod. Phys.* **25**, 269 (1953).
- <sup>10</sup>P. W. Anderson, *J. Phys. Soc. Jpn.* **9**, 316 (1954).
- <sup>11</sup>R. Kubo and K. Tomita, *J. Phys. Soc. Jpn.* **9**, 888 (1954).
- <sup>12</sup>A. Abragam, *The Principles of Nuclear Magnetism* (Oxford University Press, London, 1961).
- <sup>13</sup>H. Abe and K. Ono, *J. Phys. Soc. Jpn.* **11**, 947 (1956).
- <sup>14</sup>I. Servant, J. S. Bissey, and M. Maini, *Physica (Utrecht)* **106B**, 343 (1981).
- <sup>15</sup>D. E. Billing and B. J. Hathaway, *J. Chem. Phys.* **50**, 1476 (1969); B. J. Hathaway and D. E. Billing, *Coord. Chem. Rev.* **5**, 143 (1970).
- <sup>16</sup>D. Kivelson and R. Neiman, *J. Chem. Phys.* **35**, 149 (1961).
- <sup>17</sup>J. H. Van Vleck, *Phys. Rev.* **74**, 1168 (1948).
- <sup>18</sup>L. P. Kadanoff and P. C. Martin, *Ann. Phys. (NY)* **24**, 419 (1963).
- <sup>19</sup>R. E. Dietz, F. R. Merrit, R. Dingle, D. Hone, B. G. Silbernagel, and P. M. Richards, *Phys. Rev. Lett.* **26**, 1186 (1971).
- <sup>20</sup>P. M. Richards and M. B. Salamon, *Phys. Rev. B* **2**, 32 (1974).
- <sup>21</sup>R. D. Willet, F. J. Jardine, R. J. Wong, C. P. Landee, and M. Numata, *Phys. Rev. B* **24**, 5372 (1981).
- <sup>22</sup>R. D. Willet and F. Waldner, *J. Appl. Phys.* **53**, 2680 (1982).
- <sup>23</sup>T. Moriya, *Phys. Rev.* **120**, 91 (1960).
- <sup>24</sup>Z. G. Soos, K. T. McGregor, T. T. P. Cheung, and A. J. Silverstein, *Phys. Rev. B* **16**, 3036 (1977).